

Therapeutic potency of substituted chromones as Alzheimer's drug: Elucidation of acetylcholinesterase inhibitory activity through spectroscopic and molecular modelling investigation

Prayasee Baruah¹, Mostofa Ataur Rohman¹, Semen O. Yesylevskyy², Sivaprasad Mitra^{1*}

¹ Centre for Advanced Studies in Chemistry, North-Eastern Hill University, Shillong – 793 022, India

² Department of Physics of Biological Systems, Institute of Physics of the National Academy of Sciences of Ukraine, Prospect Nauky 46, 03028 Kyiv, Ukraine

Article Info



Article Type:

Original Article

Article History:

Received: 21 Aug. 2018
 Revised: 13 Nov. 2018
 Accepted: 17 Nov. 2018
 ePublished: 8 Mar. 2019

Keywords:

Acetylcholinesterase inhibition,
 AD drug,
 Chromones,
 PAS binding,
 Stacking interactions,
 Thioflavin T fluorescence

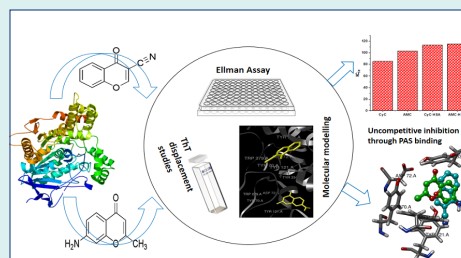
Abstract

Introduction: Documentation on the potency of chromones as acetylcholinesterase (AChE) antagonists has paved the way for the design and usage of new chromone analogues as inhibitors of AChE modelled on the hypothesis based on cholinergic pathway of Alzheimer's disease (AD). Here, 2 minimally substituted chromones, namely 3-cyanochromone (CyC) and 7-amino-3-methylchromone (AMC), were checked for their AChE inhibition efficacies and plasma protein modulation.

Methods: Colorimetric enzymatic assay as well as fluorescence measurements were performed for obtaining the experimental results, which were further corroborated by molecular docking and simulation studies.

Results: The investigated systems exhibited strong inhibition activities against AChE, with CyC ($IC_{50} = 85.12 \pm 6.70$ nM) acting as better inhibitor than AMC ($IC_{50} = 103.09 \pm 11.90$ nM) and both having IC_{50} values in the range of FDA approved cholinergic drug Donepezil ($IC_{50} = 74.13 \pm 8.30$ nM). Non-competitive inhibition was observed in both the cases with the inhibitors binding near the peripheral anionic site (PAS) of the enzyme. Having one planar nitrile group in CyC as compared to sp^3 hybridised substituents in AMC facilitated stacking interactions in the former, accounting for its higher inhibitory efficacy. A significant decrease in the inhibition potency of CyC (~32%) was noted in comparison with AMC (~5%) when the experiments were performed in presence of human serum albumin (HSA) instead of pure aqueous buffer.

Conclusion: This comparative study affirms the importance of meticulous substitution in the chromone scaffold to promote maximum inhibition potency, while considering their usage as AD drugs.



Introduction

Chromones, which are 1-benzopyran-4-one ring systems, are renowned for their miscellany of therapeutic properties.¹⁻⁶ Chromones act as exceptional prototypes for modifications based on structural changes and chemical substitutions, which pave the way for synthesis of varied compounds with a multitude of different pharmacological utilities.⁴ Because of this, they are considered vital in the world of medicine and deemed as an advantageous framework for drug discovery.^{7,8} Along with numerous

applications, they have been known to exhibit agonistic effects towards the activity of acetylcholinesterase (AChE), which is an extremely effectual enzyme and a part of the central nervous system (CNS). Experiments testing the effect of chromones on AChE peaked up with the observation of ensaculin^{9,10}; a coumarin derivative which is an isomer of chromones, inhibiting AChE activity to significant proportions.

AChE causes the depletion of acetylcholine (ACh), which is a transmitter in the CNS, by rapid hydrolysis decline, which is significant in the progression of

*Corresponding author: Sivaprasad Mitra, Email: smitra@nehu.ac.in



Alzheimer's disease (AD), a neurodegenerative symptom which usually culminates in dementia and is the reason for the alarming worldwide statistics of the same.¹¹⁻¹⁴ Therefore, cholinesterase inhibitors, which retard the activity of AChE, subsequently increasing the ACh levels in the brain, have been deliberated as characteristic treatment for this rapidly escalating disease.^{15,16} However, treatment options being symptomatic, an extensive search is on for developing new drugs with enhanced therapeutic effectiveness.

There exist quite a number of recent references that show the AChE inhibitory effects of coumarin isomers and their derivatives. In this context, several 3-formylchromone derivatives, with very promising AChE inhibitory activities, have been synthesized by Parveen et al.¹⁷ Through a multi-target-directed ligand strategy, some chromone-based compounds have been synthesized which can exhibit plural biologically relevant activities.¹⁸ Novel chromones like 2-carboxamidoalkylbenzylamines have been developed by Liu et al¹⁹ as AChE inhibitors showing inhibitory efficiency in the sub-micromolar concentration range (the lowest with $IC_{50} = 0.07 \mu M$), with some compounds possessing higher selectivity for AChE over butyl cholinesterase (BuChE). These compounds also demonstrated perceptible inhibition of the aggregation of amyloid- β ($A\beta$) fibrils through self- as well as Cu^{2+} -induction, another important pathway in the hypothesis of AD.²⁰ Recently, some chromone derivatives from Agarwood have also been developed and tested to be potent AChE inhibitors.²¹

Pertinent to general observation, coumarin analogues have been identified to associate with AChE at a site different from the substrate binding site, known as the peripheral anionic site (PAS).²² Judicious substitution with amine functional groups using appropriate spacer may amend the binding sites, in turn facilitating superior interaction with AChE and transforming them into more potent inhibitors.²³⁻²⁵ Hence, identifying the site and mode of inhibition deems vital in AChE inhibition.

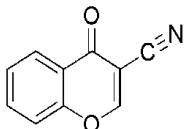
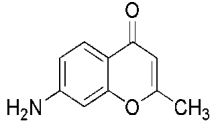
In the passageway of drugs in the body, many of them associate with blood constituents, mainly plasma proteins,

wherein only that fraction of the total amount which is not bound remains accessible for dispersing out of the vascular structure to the targeted locations for therapeutic efficacy.²⁶ In fact, the role of serum proteins in modulating the inhibitory efficacies of targeted drugs and the importance of considering the behaviour of inhibitors in presence of serum matrix as a potential screening test for AD drugs was reported in earlier communications from this laboratory.²⁷ Therefore, a comparison on the activities of potential drugs in buffer and human serum albumin (HSA) seems important while screening potential drugs.

In connection with AD, blood plasma proteins like HSA have portrayed the ability of controlling the aggregation of $A\beta$ by controlling the equilibrium of $A\beta$ peptide through the blood brain barrier.^{28,29} Reports on 2 groups of patients, one with higher level of serum albumin and the other with lower level suggested better cognizance and reasoning performance in the former over the latter.^{30,31} Three homologous domains (named I, II, and III) form the core of HSA's structural organisation, each comprised of 2 distinct helical subdomains (named A and B) which are joined together by a loop.³² HSA, on account of its modular arrangement, consists of many different sites which facilitate ligand binding. It, however, encompasses 2 sites with higher affinity for binding of ligands called Sudlow's sites I and II located in Subdomain IIA and IIIA, respectively.³³

In this report, 2 chromone derivatives, one containing a methyl group and a primary amine in its chromone skeleton (7-amino-2-methylchromone, AMC) and the other possessing a tertiary amine moiety (3-cyanochromone, CyC), the structures and other relevant parameters of which have been depicted in Table 1, have been tested for their AChE inhibition capabilities. The modulation of inhibitor potency in HSA medium has also been quantified. The affirmative experimental results of these 2 simple chromone prototypes imply the benefits of designing new drugs with the chromone scaffold as a backdrop and validating several structure activity relationship (SAR) reviews pertaining to the enzyme inhibitory capacities of chromones.

Table 1. Structures and relevant pharmacological parameters for the tested systems

Name	Structure	Molecular weight (g mol ⁻¹)	Log p	TPSA (Å ²)
3-cyanochromone (CyC)		171.15	1.50	54.00
7-amino-2-methylchromone (AMC)		175.18	1.00	56.23

Materials and Methods

Chemicals

The reagents used in the present study were of highest quality analytical grade, which were used as received. AMC and CyC were procured from Sigma Aldrich, Germany (cat. No. 383481 and 30779705, respectively). AChE from *Electrophorus electricus* (electric eel) (cat. No. C2888), acetylthiocholine iodide (cat. no. A5751), Donepezil hydrochloride monohydrate (cat. no. D6821), and thioflavin T (ThT, cat. No. T3516) were all purchased from Sigma Aldrich, Germany. Dithiobis (2-nitrobenzoic acid) was received from Sisco Research Laboratories (SRL, India) (product NO. 32363) and HSA (Cat. No. 10878) was purchased from Sigma Aldrich, Germany, in a lyophilized powder form. The experiments were performed in analytical grade type II water of ~10 MΩ cm resistivity (at 298 K), obtained from Elix 10 (Millipore India Pvt. Ltd) water purification system. The pH of the buffer solutions were checked by Systronics μ-pH system 361.

Kinetic characterization of AChE activity

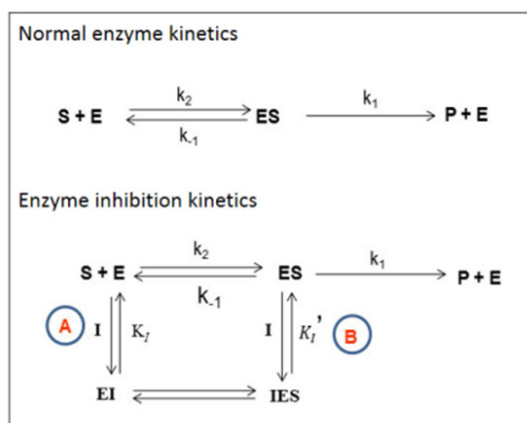
Ellman method with slight modification was used for assaying the activity of AChE in phosphate buffer of pH = 8.0 (0.1 M) at 298 K and for its kinetic characterization.³⁴ The details of the experimental procedure is given in supplementary section ST1. The scheme for the basis of the enzyme kinetics is shown in Scheme 1.

Equation 1 gives the initial rate (v_0) of the hydrolysis reaction:

$$v_0 (\text{moles l}^{-1}\text{s}^{-1}) = \frac{\text{Slope}(\text{absorbance s}^{-1})}{\varepsilon \times l} \quad \text{Eq. (1)}$$

where ε represents the absorption coefficient of the yellow anion, l is the path length (= 0.442 cm³⁵).

Non-linear regression analysis of v_0 against initial substrate concentration (S_0) gave the values of the Michaelis-Menten (MM) constant, K_m and maximum hydrolysis rate, V_{\max} in the normal and enzyme inhibition cases using Eq. 2 and Eq. 3, respectively.³⁶



Scheme 1. The Michaelis-Menten (MM) scheme for enzyme inhibitory kinetics. A and B represent different inhibition pathways.

$$v_0 = \frac{V_{\max} [S_0]}{K_m + [S_0]} \quad \text{Eq. (2)}$$

$$v_0 = \frac{V_{\max} [S_0]}{K_{m'} + [S_0]} \quad \text{Eq. (3)}$$

where, $V_{\max'} = \frac{V_{\max}}{\alpha'}$, $K_{m'} = \frac{\alpha}{\alpha'} \times K_m$, or $K_{m'} = \alpha \times K_m$ (representing path A only for inhibition);

$\alpha = 1 + \frac{[EI]}{[E]}$ and $\alpha' = 1 + \frac{[IES]}{[ES]}$ (representing both paths A and B).

The characteristic IC_{50} parameter for inhibition in both the media were obtained from the modified Hill relation (Eq. 4).³⁷⁻³⁹

$$\frac{\Delta V}{\Delta V_{\max}} = \frac{[I]^{n_H}}{K_{0.5}^{n_H} + [I]^{n_H}} \quad \text{Eq. (4)}$$

where ΔV is the initial rate decrease observed in presence of a definite concentration of inhibitor $[I]$, ΔV_{\max} represents maximal initial velocity decrease, $K_{0.5}$ which is pharmacologically equivalent to IC_{50} , the inhibitor concentration to induce half-maximal change in the initial velocity. The term n_H represents the Hill coefficient.

Fluorescence measurements

All steady state fluorescence studies were carried out in Quanta Master (QM-40) apparatus (Photon Technology International, PTI), the details of which have been given in supplementary section ST2. The following relation was used to obtain the corrected fluorescence intensity after removal of the inner filter effect⁴⁰

$$F^{Corr}(\lambda_E, \lambda_F) = F_{Obs}(\lambda_E, \lambda_F) \times \frac{A(\lambda_E)}{A_{tot}(\lambda_E)} \quad \text{Eq. (5)}$$

Here, the absorbance of the free ThT is given by A and A_{tot} represents the total absorbance of the solution at λ_E , which is the experimental excitation wavelength.

Molecular dynamics simulation and docking calculation

Molecular docking calculations were performed for a deeper understanding of the binding of the inhibitors to the macromolecules. After retrieval of the 3D structures of AChE (PDB ID: 1C2B) and HSA (PDB ID: 1AO6) from Protein Data Bank (<http://www.rcsb.org>), they were made suitable for docking by eliminating all heteroatoms, water molecules, and ions. The ligand structures were fully optimized with density functional theory at B3LYP/6-311++g (d,p) levels as incorporated in Gaussian 09 platform.

Recent molecular dynamics (MD) simulation results revealed the crystal structure of AChE protein to be significantly different from its equilibrium structure in the solvent.⁴¹ In this work, extensive MD simulations were carried out on the protein structure in aqueous medium to equilibrate it. Gromacs 5.1.2 package was used for the simulations,⁴² utilizing AMBER99SB force field. The

curtailed dodecahedron box used for counterbalancing the protein's negative charge contained ~13500 TIP3P water molecules and 9 Na⁺ ions. Solvated system was energy minimized using the methodology of the steepest descent algorithm. Temperature and pressure were kept constant at 310 K and 1 bar, respectively, throughout the course of production simulations. Velocity rescale thermostat⁴³ and Berendsen barostat⁴⁴ were used for maintaining the temperature and pressure, respectively. PME method was used for long state electrostatics and 2 fs was used as the integration step⁴⁵ with Verlet cutoff.⁴⁶ The system was simulated for 465 ns. The equilibration was monitored by RMSD of protein in respect to its initial conformation.

It is to be noted that AChE exhibits large conformational changes in water in comparison to crystal structure. Therefore, the backbone RMSD is more relevant than RMSD of heavy atoms; because it reflects the stabilization of the tertiary and secondary structures reliably without any noise introduced by the motion of side chains. That is why the backbone RMSD was used in evaluating the protein equilibration (Fig. S1). It is clear that the RMSD stabilizes only after approximately 400 ns of simulation. Thus, only last 65 ns of the trajectory were considered equilibrated and used for subsequent docking simulations. One hundred thirty frames were extracted with the step of 0.5 ns from equilibrated part of the trajectory. The structures aligned by their peptide backbones, thus obtained, were taken to represent the ensemble of all solvated protein conformations. All docking took place inside a volume of 25 Å³ which was at the middle of the center of masses of the residues 70, 72, 121, 279, and 334. The MD trajectory was evidence of the flexibility of the protein and the reason the protein was fixed for all dockings.

In the case of HSA, all-atom MD trajectory of 100 ns of pre-equilibrated protein in water was utilized as per standard protocol.⁴⁷ In this case, 200 frames were extracted from this trajectory and the docking volume of 40 Å³ was centered at the center of masses of the residues 134, 186, 123, 117, 161, 138, 165, 138, 161, and 157 as suggested by blind docking in the case of HSA.

All structures to be docked were fashioned using MGLTools-1.5.6 software whereas the default protocol of Autodock Vina⁴⁸ was used for the actual docking. The docked poses were fashioned using Chimera⁴⁹ and Ligplot.⁵⁰ Pteros 2.0 molecular modeling library was the base of the analysis of docking results.⁵¹ Five top-ranked poses were recorded for each docking simulation. VMD 1.9.3⁵² was used for visualization purposes.

Results

Physico-chemical properties and comparative AChE inhibition activity of the investigated systems

All the relevant physico-chemical parameters for the investigated systems have been depicted in Table 1. The logP and total polar surface area (TPSA) values of

the chromones were calculated using Molinspiration cheminformatics software (<https://www.molinspiration.com>) and found to be 1.50 and 1.00 for CyC and AMC, respectively. The corresponding TPSA values were 54.00 and 56.23 Å² respectively.

The performed kinetic experiments revealed the inhibition to be a non-competitive one. This type of inhibition falls under the category of mixed inhibition, and as per the defining characteristics of non-competitive inhibition, here only the V_{\max} suffered a decrease. On the other hand, K_m remained practically unaltered (Table 2). Here, the values of α and α' were found to be identical. The MM and LB plots (Fig. 1, (ia) and (ic), respectively) show that the reduction in V_{\max} is higher in case of CyC, which was further verified by the estimation of IC_{50} values of individual systems described later. The cholinergic drug, DON, which was used as a control in our experiment showed comparable kinetic parameters that matched the previously published reports.²⁷ All experimental results of DON have been supplied in the supplementary section (Figs. S2-S4).

ThT displacement studies

The fluorescence intensities of ThT-AChE system suffer considerable hypochromic shifts on addition of gradually surging amounts of the investigated compounds. The quenching of fluorescence was quantitatively analysed using the Stern-Volmer (SV) equation. The greater binding in case of CyC is demonstrated with its higher K_{sv} value ($3.7 \times 10^5 \text{ M}^{-1}$) in comparison to that of AMC ($2.3 \times 10^5 \text{ M}^{-1}$). The fluorescence emission quenching spectra as well as the SV plot for CyC are depicted in Fig. 2. The corresponding plots for AMC are shown in Fig. S5.

Modulation of inhibitory potency in HSA matrix

All experiments were carried out under fixed HSA concentration (ca. 250 mM), which is in the range of its reported functional quantity in the body.⁵³ Higher modulation was observed in case of CyC than AMC with a greater reduction in V_{\max} value, as seen in Fig. 1(ii), as well as significant alteration in IC_{50} values, as obtained from Hill analysis (Fig. 3). The IC_{50} values obtained in aqueous buffer medium proved CyC to be more potent inhibitor ($IC_{50} = 85.12 \pm 6.7 \mu\text{M}$) and shows the value quite close to the used standard, DON ($IC_{50} = 74.13 \pm 5.6 \text{ nM}$); while, AMC possessed an IC_{50} value of $103.09 \pm 11.9 \text{ nM}$ (Table 2). In HSA medium, the IC_{50} changed to $113.43 \pm 4.5 \text{ nM}$ and $115.11 \pm 12.2 \text{ nM}$ for CyC and AMC, respectively.

The mechanistic pathway for the enzyme inhibition was the same for AChE in both the experimental media (buffer and HSA), as apparent from the MM and LB plots depicted in Fig. 1 (iia and iic, respectively).

The following equation gives a quantitative estimation of the relative percentage of difference of inhibitor potencies on changing the experimental medium²⁷:

Table 2. List of kinetic parameters for enzymatic reaction at varying concentrations of inhibitor in aqueous buffer media

Inhibitor	$K_m/\mu\text{M}$	V_{max}/nMs^{-1}	α	α'	$IC_{50} (\text{nM})$	n_H
	Michaelis-Menten parameters			Hill parameters		
AChE in CyC						
[CyC] = 0 nM	174 ± 15 (177±20)	825 ± 24 (841±20)	1.0 (1.0)	1.0 (1.0)		
[CyC] = 5 nM	172 ± 20 (178±25)	631 ± 21 (730±17)	1.3 (1.1)	1.3 (1.1)	85.12 ± 6.7 (113.43±4.6)	1.51 ± 0.1 (1.89±0.17)
[CyC] = 10 nM	180 ± 23 (179±19)	538 ± 31 (671±30)	1.5 (1.2)	1.5 (1.2)		
AChE in AMC						
[AMC] = 0 nM	149 ± 14 (146±35)	793 ± 23 (798±23)	1.0 (1.0)	1.0 (1.0)		
[AMC] = 5 nM	148 ± 18 (150±38)	670 ± 26 (711±47)	1.2 (1.2)	1.2 (1.2)	110.64 ± 12.1 (115.11±12.2)	1.45 ± 0.1 (1.52±0.1)
[AMC] = 10 nM	155 ± 36 (179±27)	560 ± 39 (557±39)	1.4 (1.5)	1.4 (1.4)		
AChE in DON						
[DON] = 0 nM	146 ± 28 (140±32)	793 ± 47 (794±59)	1.0 (1.0)	1.0 (1.0)		
[DON] = 5 nM	160 ± 36 (163±38)	550 ± 48 (625±42)	1.4 (1.4)	1.4 (1.4)	74.13 ± 5.6 (110.64±12)	1.45 ± 0.1 (1.51±0.1)
[DON] = 10 nM	138 ± 13 (140±26)	484 ± 15 (571±35)	1.5 (1.4)	1.6 (1.4)		

^a AChE = 0.079 units/mL.

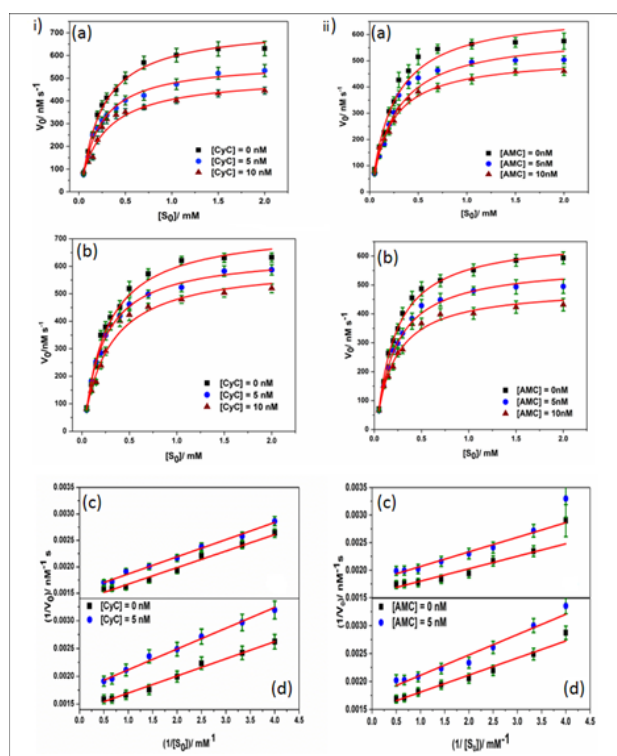


Fig. 1. Hydrolysis curve (scattered points) (a, b) and Lineweaver-Burk (LB) plots (c,d) for the AChE hydrolysis data in aqueous buffer of pH 8.0 (a, c) and HSA medium (b, d) in absence and presence of different concentrations of CyC (1) and AMC (2). The solid line in hydrolysis curves represents non-linear regression of the experimental data points. [AChE] = 0.079 u/mL.

$$\Delta' IC_{50} (\%) = \frac{IC_{50}(HSA) - IC_{50}(Buffer)}{IC_{50}(Buffer)} \times 100 \quad \text{Eq. (6)}$$

which was found to be 32% and a mere 5% for CyC and AMC, respectively. The significant difference between the modulation of CyC and AMC inhibition activity in HSA medium is worth noting and has been discussed in detail in the later section.

To show the differences in IC_{50} between the various systems and measure how large a difference holds

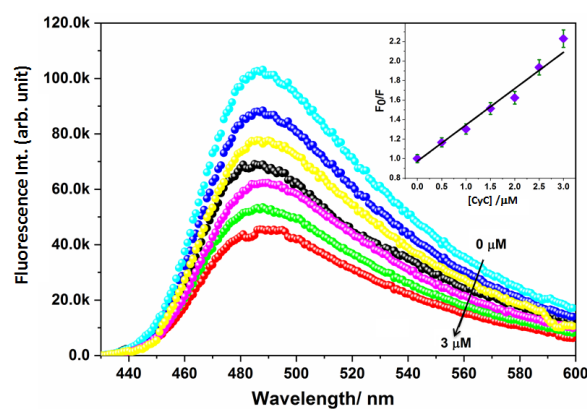


Fig. 2. Quenching of emission intensity of ThT-AChE binary system in the presence of increasing concentrations of CyC (left) and the corresponding Stern-Volmer (SV) plot (right).

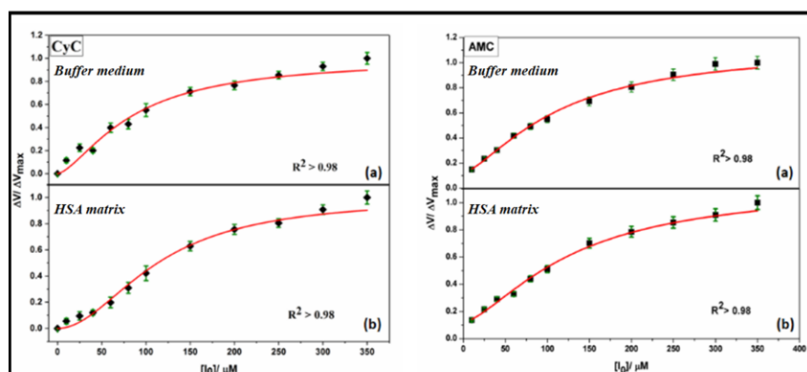


Fig. 3. Modified Hill analysis of AChE inhibition in aqueous buffer (a) and HSA medium (b) of CyC and AMC.

significance, the standard student t-test (details of which has been described in supplementary section ST3) was used as a measure of statistical hypothesis.⁵⁴ The t-value (given in Table S1, See Supplementary file 1) was found to be more than 0.05 in all cases, signifying a significant difference. The df value, was found to be 70 for 12 data points in each set.

Molecular modelling results

The docking scores for both ligands are distributed across a significant range due to different protein structures present in the ensemble of equilibrium conformations, as shown in Fig. 4. It is evident that CyC has a much better maximal binding score of -31.79 kJ/mol, in comparison with -29.28 kJ/mol for AMC in the case of AChE. Distribution of the maximum binding score for CyC is -25.52 kJ/mol in comparison to -24.68 kJ/mol for AMC, and the whole distribution for CyC is shifted to lower binding score values in the case of AChE. The docking results (Table 3) give the energies of both the chromones

to be in the range of ThT (-31.31 kJ/mol), represented in Table S2. The best docked poses of the ligands with AChE is depicted in Fig. 5, where the Ligplots reveal the closer contact with the residues of PAS than with those of AMC. To find more about the pi-pi stacking interactions, Achilles Server was used (<http://bio-hpc.eu/software/blind-docking-server/>).⁵⁵

In the case of HSA, the maximal binding scores for both ligands were the same (-30.96 kJ/mol). Very similar trend was also observed for HSA as with AChE but the maximum distributions were shifted to the right by approximately 0.42 kJ/mol. The best docked poses of the ligands with HSA are depicted in Fig. S6. All results corresponding to the best docked pose are given in Table 3. On the other hand, the energy of other poses is listed in Table S3.

Discussion

Several molecular properties including molecular weight, lipophilicity (logP), and TPSA are widely used

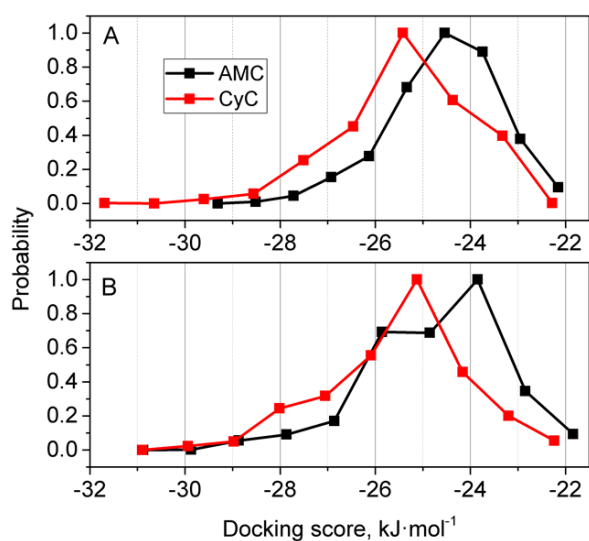


Fig. 4. Normalized distributions of binding scores for docking of AMC and CyC to the ensembles of conformations of AChE (A) and HSA (B) proteins.

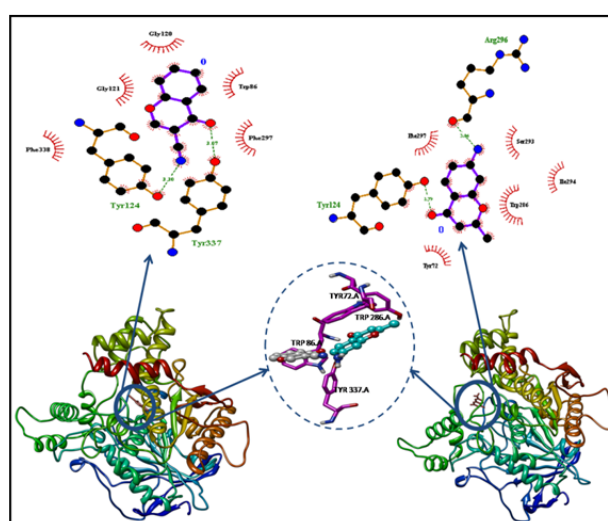


Fig. 5. Docked poses of CyC (left) and AMC (right) with AChE. The binding site has been magnified to depict different binding poses of CyC (grey) and AMC (aqua blue) with the neighbouring residues.

Table 3. Affinities of the most stable docked pose of the inhibitors with AChE and HSA from molecular docking calculations

Receptor	Ligand	Binding affinity (kJ/mol)	K _i (μM)	H-bonded residues	Hydrophobic interactions
AChE	CyC	-35.02	0.9859	Tyr 124, Tyr 337	Phe 338, Gly 124, Gly 120, Trp 86, Phe 297
AChE	AMC	-33.37	0.9866	Tyr 124, Arg 296	Tyr 72, Trp 286, Ser 293, Phe 297, Ile 294
HSA	CyC	-34.60	0.9861	Nil	Arg 186, Arg 117, Met 123, Tyr 161, Phe 165, Leu 182, Ile 142, Tyr 138, Phe 134
HSA	AMC	-32.96	0.9867	Nil	Phe 134, Phe 165, Met 123, Ile 142, Tyr 138, Tyr 161, Leu 135, Leu 139, Ala 158, Phe 157, Leu 154

as important parameters in modern drug discovery. Lipophilicity is an important physicochemical property for evaluating the capacity of a drug for passing through the blood-brain barrier (BBB). The optimal logP value for efficacious permeation of CNS was reported to be ca. 2 ± 0.7 ; whereas, TPSA cut-off value was determined to be $< 90 \text{ \AA}^2$ for potential drugs.⁵⁶ For FDA approved drugs, the molecular weight was determined to be ideally less than 450 g/mol.⁵⁷ The logP and TPSA values of the drugs (1.50 and 1.00 Å^2 for CyC, and 54.00 and 56.23 Å^2 for AMC) implied that the drugs were lipophilic enough to cross BBB and had optimum TPSA to be considered as potential drugs.

The calculated logP value of AMC was lower than the optimal value reported for CNS penetrated drugs. However, it is to be noted that although logP is an important parameter for prediction and optimisation, the suitability of a CNS drug does not depend only on this quantity. Several other factors like low molecular weight, TPSA $< 90 \text{ \AA}^2$, number of heteroatoms < 5 , and ability to form hydrogen bonds also contribute to the drug efficacy. Except for logP being lower than the prescribed value in case of AMC, all other parameters fall within the suitable range for both the studied chromones, rendering their suitability as possible CNS drugs.

When tested via the Ellman method, both the chromones were found to exhibit inhibitory activity against AChE with the experimental assessment revealing CyC to be the more potent inhibitor (Table 2). In the non-competitive pathway, binding of the inhibitor to either the enzyme or the enzyme-substrate complex is equally plausible, meaning that the pathways A and B in Scheme 1 have equal probability of occurrence, rendering α and α' to be equal. Here, the inhibitor binds to an allosteric site, which is different from the primary substrate binding site.³⁷ In case of AChE, the non-competitive way is linked with PAS,⁵⁸ which is also confirmed by molecular docking results discussed later. The estimated IC₅₀ values indicate that both the chromones showed inhibitory efficiency akin to the reference drug DON. However, experiments on 2 coumarin derivatives reported elsewhere⁵⁹ revealed that replacement of the coumarin moiety with chromones results in a loss of inhibitory efficiency. Similar observation has already been reported in several SAR reviews and

it is well-known that coumarin derivatives normally show better inhibition potency toward AChE activity in comparison with their chromone counterparts.^{23,60} However, a noteworthy feature of this study is that both the present systems, with the slightest substitution in the chromone moiety, exhibit an inhibitory efficacy comparable and, even in some cases, greater than other generously substituted chromone derivatives reported in the literature.^{17-19,21}

The emission intensity of ThT, a probe that binds selectively to the PAS of AChE, has been known to increase multi-fold when bound to AChE, as seen in this case (Fig. 2 and Fig. S5).⁶¹ The change in intensity of this ThT-bound AChE fluorescence in the presence of inhibitors can be used as an assay for quantifying the inhibitory potencies of cholinergic drugs.⁶² The results obtained signifies greater inhibitory effectiveness of CyC, which is in conformity with kinetic experiments discussed above; as percentage of ThT fluorescence quenching is a direct manifestation of inhibitory efficiency.⁶³ The quenching of fluorescence intensity can be perceived because of displacement of ThT from the AChE gorge by the inhibitors,⁶⁴ resulting in a significant reduction of the emission intensity.

When HSA was used as a modulatory medium, the reason behind the reduction of inhibitory efficacy of the compounds could be ascribed to the confiscation of the chromones by HSA. This sequestration, in turn, results in diminution of the unbound fraction of drug to bind with the enzyme. Thus, greater affinity for HSA, as also verified by molecular docking calculation, results in greater reduction of inhibitory potency of CyC in HSA. The *t* values demonstrated that the difference in the IC₅₀ values of all the systems were significant. This represents the modulation of the inhibitory potency between the 2 systems in buffer as well as while switching the medium to HSA.

Structurally, AChE consists of a narrow and deep gorge, spanning 20 Å in length. The substrate binding site is the catalytic active site (CAS), which along with an allosteric site called PAS compose the 2 ends of the gorge; the CAS being near the bottom and the PAS residing at the surface.^{57,65} In case of eeAChE, the catalytic site is comprised of a triad of Ser203, His447, Glu334, whereas the PAS consists of 4 amino acids: Trp86, Tyr337, Trp286,

and Tyr72.⁶⁶ PAS inhibitors occlude the admittance of substrates and exodus of products from the enzyme's active site, causing steric obstruction and allosteric variation.^{25,67}

Since both the chromones have an ability to form H-bonds (a nitrile group in CyC and a primary amine in AMC), the variance in their binding affinities cannot be hypothesized to be an inference of the stability caused by H-bonding alone. The role of pi-pi stacking interactions of the drugs with aromatic residues of AChE (especially Trp and Tyr) in inhibition of enzyme AChE as well as BuChE have been documented.⁶⁸ CyC that contains a linear cyano group owing to tertiary nitrogen atom, can be considered as a planar molecule and can stack parallel with aromatic residues, facilitating stacking interactions. On the other hand, AMC that contains a methyl (-CH₃) as well as a primary amine (-NH₂) group do not exhibit planarity due to the tetrahedral shape of the substituents. These enhanced stacking interactions in case of CyC may be the cause of its higher inhibitory efficiency towards AChE.

The docking results suggests that in average CyC binds better to the specified binding site of AChE in comparison to AMC and this result stands for different protein conformations found in equilibrium ensemble in water. This observation is concurrent with the experimental observation of superior inhibitory activity of CyC over AMC. However, CyC also binds better to the selected region of HSA in comparison to AMC, demonstrating higher degree of sequestration in case of the former. Therefore, a significant fraction of CyC becomes unavailable to demonstrate AChE inhibition in albumin matrix and causes relatively large deviation in IC₅₀ parameter in comparison with buffer medium. The association propensities for the ligands are surprisingly similar in both AChE and HSA, which suggests that the binding of the studied ligands to these proteins might be highly concurrent.

The simulation results confirm CyC and AMC to be PAS-binding ligands as that of ThT, thereby proving the ease of displacement as discussed previously. The results obtained from Achilles Blind Docking validated our hypothesis of pi-pi stacking since CyC had stacking interactions both with Trp 86 and Phe 295, whereas AMC had stacking interactions only with Trp 86, because of structural constraints. Further justifying the concept of stacking interactions may play an important role in inhibition potency (Fig. S7).

Conclusion

The discovery and design of curative therapies for AD is an exigent task owing to the elusive understanding of its causative mechanisms. Due to the limited effectiveness of the available drugs as well as the side effects, designing new AChE inhibitors with greater effectiveness is the need of the hour. The investigated chromones used in this study, CyC and AMC, possess pertinent lipophilicity

Research Highlights

What is current knowledge?

- ✓ AChE inhibitors are used as therapeutic agents in the treatment of AD.
- ✓ Coumarins and chromones have been found to have AChE antagonistic property

What is new here?

- ✓ Minimum albeit judicious substitution in the chromone scaffold helps to attain maximum inhibition efficiency.
- ✓ Binding with HSA medium and replacement of ThT have been further established as standard pre-screening AD drug tests.
- ✓ Validity of computational studies has been checked in the periphery of enzymatic and fluorimetric assays.
- ✓ The site and mode of binding with AChE and plasma protein plays an important role in the pharmacological efficacy of potential AD drugs.

as well as TPSA values and exhibit substantial inhibitory efficiency on AChE. CyC showed higher potency of inhibition, probably due to the enhanced facility for pi-pi stacking interactions owing to the presence of a planar tertiary amine group. CyC also showed higher modulation in HSA medium. The modulation in serum albumin matrix re-instates the significance of taking the delivery medium into consideration for screening potential AD drugs. The chromones displaced Thioflavin-T from the AChE binding site and bound non-competitively with AChE at the PAS. A comparison of the anti-cholinesterase potencies of these chromones amplify the probability of the usage of chromones, even with minimal albeit prudent fabrication of its skeleton in acting as possible cholinergic drugs in the Alzheimer's treatment.

Acknowledgement

The authors thank Prof. K. Aguan of Department of Biotechnology and Bio-informatics, NEHU for many helpful discussions.

Funding sources

The research was financially supported by the Department of Biotechnology (BT/232/NE/TBP/2011) and Department of Science and Technology (SR/FST/CSI194/2008), Govt. of India.

Ethical statement

There is none to be disclosed.

Competing interests

No conflicting interests are to be declared.

Authors' contribution

Planned the experiments: PB, SM; executed the experiments: PB, MAR; data analysis: PB, MAR; supplied the chemicals and analysis tools: SM; manuscript writing: PB, SOY, SM; docking and MD simulation: SOY.

Supplementary Materials

Supplementary file 1 contains Figs. S1-S7 and Tables S1-S3.

References

1. Tawfik HA, Ewies EF, El-hamouly WS. Synthesis of chromones and

- their applications during the last ten years. *Int J Res Pharm Chem* **2014**;4 (4): 1046–1085.
- Nawrot-Modranka J, Nawrot E, Graczyk J. In vivo antitumor, in vitro antibacterial activity and alkylating properties of phosphorohydrazine derivatives of coumarin and chromone. *Eur J Med Chem* **2006**;41 (11): 1301–1309. doi: 10.1016/j.ejmech.2006.06.004
 - Marques NFLM, Marques M PM. Bioactive Chromone Derivatives – Structural Diversity. *Current Bioactive Compounds*. **2010**; 6 (2):76–89. doi: 10.2174/157340710791184859
 - Reis J, Gaspar A, Milhazes N, Borges F. Chromone as a Privileged Scaffold in Drug Discovery: Recent Advances. *J Med Chem* **2017**;60 (19): 7941–7957. doi: 10.1021/acs.jmedchem.6b01720
 - Augstein J, Cairns H, Hunter D, Lee TB, Suschitzky J, Altounyan REC, et al. New Orally Effective Chromone Derivatives for the Treatment of Asthma. *Agents Actions*. **1977**;7 (4): 443–445. doi: 10.1007/BF01966850
 - Edwards AM, Howell JBL. The chromones: history, chemistry and clinical development. *Clin Exp Allergy* **2000**;30 (30): 756–774. doi: 10.1046/j.1365-2222.2000.00879.x
 - Gaspar A, Matos MJ, Garrido J, Uriarte E, Borges F. Chromone: a valid scaffold in medicinal chemistry. *Chem Rev* **2014**;114(9): 4960–4992. doi: 10.1021/cr400265z
 - Keri RS, Budagumpi S, Pai RK, Balakrishna RG. Chromones as a privileged scaffold in drug discovery: a review. *Eur J Med Chem* **2014**;78: 340–374. doi: 10.1016/j.ejmech.2014.03.047
 - Hilgert M, Nöldner M, Chatterjee SS, Klein J. KA-672 inhibits rat brain acetylcholinesterase in vitro but not in vivo. *Neurosci Lett* **1999**;263 (2–3): 193–196. doi: 10.1016/S0304-3940(99)00149-4
 - Hoerr R, Noeldner M. Ensaculin (KA-672 HCl): a multitransmitter approach to dementia treatment. *CNS Drug Rev* **2002**;8(2): 143–158. doi:10.1111/j.1527-3458.2002.tb00220.x
 - Martyn JA, Fagerlund MJ, Eriksson LI. Basic Principles of neuromuscular transmission. *Anaesthesia* **2009**;649(suppl 1): 1–9. doi: 10.1111/j.1365-2044.2008.05865.x
 - Francis PT, Palmer AM, Snape M, Wilcock GK. The Cholinergic Hypothesis of Alzheimer's Disease: A Review of Progress. *J Neurol Neurosurg Psychiatry* **1999**;66(2): 137–147. doi: 10.1136/jnnp.66.2.137
 - Craig LA, Hong NS, McDonald RJ. Revisiting the Cholinergic Hypothesis in the Development of Alzheimer's Disease. *Neurosci Biobehav Rev* **2011**;35 (6): 1397–1409. doi: 10.1016/j.neubiorev.2011.03.001
 - Wimo A, Guerchet M, Ali GC, Wu YT, Prina AM, Winblad B. The Worldwide Costs of Dementia 2015 and Comparisons with 2010. *Alzheimers Dement* **2017**;13 (1): 1–7. doi: 10.1016/j.jalz.2016.07.150
 - Livingston G, Sommerlad A, Orgeta V, Costafreda SG, Huntley J, Ames D. Dementia Prevention, Intervention, and Care. *Lancet* **2018**;390(10113): 2673–2734. doi:10.1016/S0140-6736(17)31363-6.
 - Alzheimer's Association. 2014 Alzheimer's Disease Facts and Figures. *Alzheimers Dement* **2014**;10(2): 1–80. doi: 10.1016/j.jalz.2015.02.003
 - Parveen M, Malla AM, Yaseen Z, Ali A, Alam M. Synthesis, Characterization, DNA-Binding Studies and Acetylcholinesterase Inhibition Activity of New 3-Formyl Chromone Derivatives. *J Photochem Photobiol B Biol* **2014**;130: 179–187. doi: 10.1016/j.jphotobiol.2013.11.019
 - Lu C, Guo Y, Yan J, Luo Z, Luo HB, Yan M, et al. Design, synthesis, and evaluation of multitarget-directed resveratrol derivatives for the treatment of Alzheimer's disease. *J Med Chem* **2013**;56 (14): 5843–5859. doi: 10.1021/jm400567s
 - Liu Q, Qiang X, Li Y, Sang Z, Li Y, Tan Z, et al. Design, Synthesis and Evaluation of Chromone-2-Carboxamido-Alkylbenzylamines as Multifunctional Agents for the Treatment of Alzheimer's Disease. *Bioorganic Med Chem* **2015**;23 (5): 911–923. doi: 10.1016/j.bmc.2015.01.042
 - Selkoe DJ, Hardy J. The amyloid hypothesis of Alzheimer's disease at 25 years. *EMBO Mol Med* **2016**;8 (6): 595–608. doi: 10.15252/emmm.201606210
 - Liao G, Mei WL, Kong FD, Li W, Yuan JZ, Dai HF. 5,6,7,8-Tetrahydro-2-(2-Phenylethyl)chromones from Artificial Agarwood of *Aquilaria Sinensis* and Their Inhibitory Activity against Acetylcholinesterase. *Phytochemistry* **2017**;139: 98–108. doi: 10.1016/j.phytochem.2017.04.011
 - Fallarero A, Oinonen P, Gupta S, Blom P, Galkin A, Mohan CG. Inhibition of acetylcholinesterase by coumarins: the case of coumarin 106. *Pharmacol Res* **2008**;58(3–4): 215–221. doi: 10.1016/j.phrs.2008.08.001
 - Anand P, Singh B, Singh N. A review on coumarins as acetylcholinesterase inhibitors for Alzheimer's disease. *Bioorganic Med Chem* **2012**;20(3): 1175–1180. doi: 10.1016/j.bmc.2011.12.042
 - Shen Q, Peng Q, Shao J, Liu X, Huang Z, Pu X. Synthesis and Biological Evaluation of Functionalized Coumarins as Acetylcholinesterase Inhibitors. *Eur J Med Chem* **2005**;40 (12): 1307–1315. doi: 10.1016/j.ejmech.2005.07.014
 - Bourne Y, Taylor P, Radić Z, Marchot P. Structural Insights into Ligand Interactions at the Acetylcholinesterase Peripheral Anionic Site. *EMBO J* **2003**;22(1): 1–12. doi: 10.1093/emboj/cdg005
 - Lohman JJHM, Merkus FWHM, Rahn KH. Plasma Protein Binding of Drugs. *Pharm. Weekbl.* **1986**;8(6): 302–304.
 - Islam MM, Gurung AB, Bhattacharjee A, Aguan K, Mitra, S. Human Serum Albumin Reduces the Potency of Acetylcholinesterase Inhibitor Based Drugs for Alzheimer's Disease. *Chem Biol Interact* **2016**;249: 1–9. doi: 10.1016/j.cbi.2016.02.012
 - Stanyon, H. E.; Viles, J. H. Human Serum Albumin Can Regulate Amyloid- β Peptide Fiber Growth in the Brain Interstitium: Implications for Alzheimer Disease. *J Biol Chem* **2012**;287(33): 28163–28168. doi: 10.1074/jbc.C112.360800
 - Milojevic J, Melacini G. Stoichiometry and Affinity of the Human Serum Albumin-Alzheimer's A β Peptide Interactions. *Biophys J* **2011**;100 (1): 183–192. doi: 10.1016/j.bpj.2010.11.037
 - Ezra A, Rabinovich-Nikitin I, Rabinovich-Toidman P, Solomon B. Multifunctional Effect of Human Serum Albumin Reduces Alzheimer's Disease Related Pathologies in the 3xTg Mouse Model. *J Alzheimers Dis* **2015**;50(1): 175–188. doi: 10.3233/JAD-150694
 - Llewellyn DJ, Langa KM, Friedland RP, Lang IA. Serum albumin concentration and cognitive impairment. *Curr Alzheimer Res* **2010**;7 (1): 91–96.
 - Petipas I, Bhattacharya AA, Twine S, East M, Curry S. Crystal structure analysis of warfarin binding to human serum albumin. anatomy of drug site I. *J Biol Chem* **2001**;276 (25): 22804–22809. doi: 10.1074/jbc.M100575200
 - Fasano M, Curry S, Terreno E, Galliano M, Fanali G, Narciso P. The extraordinary ligand binding properties of human serum albumin. *IUBMB Life* **2005**;57 (12): 787–796. doi:10.1080/15216540500404093
 - Ellman GL, Courtney KD, Andres V, Featherstone RM. A new and rapid colorimetric determination of acetylcholinesterase activity. *Biochem Pharmacol* **1961**;7 (2): 88–95. doi: 10.1016/0006-2952(61)90145-9
 - Pheifer JH, Briggs DE. The estimation of thiols and disulphides in barley. *J Inst Brew* **1995**;101(1): 5–10. doi: 10.1002/j.2050-0416.1995.tb00843.x
 - Nelson DL, Cox MM. *Lehninger Principles of Biochemistry*. 4th ed. W.H. Freeman; **2004**. p. 1119.
 - Copeland RA. Evaluation of Enzyme Inhibitors in Drugs Discovery: A Guide for Medicinal Chemists and Pharmacologists. 2nd ed. New York: John Wiley & Sons, Inc.; **2013**.
 - Chen X, Wehle S, Kuzmanovic N, Merget B, Holzgrabe U, König B, et al. Acetylcholinesterase inhibitors with photoswitchable inhibition of β -amyloid aggregation. *ACS Chem Neurosci* **2014**; 5: 377–389. doi: 10.1021/cn500016p
 - Pratap PR, Mikhaylyants LO, Olden-Stahl N. Fluorescence measurement of nucleotide association with the Na⁺/K⁺-ATPase. *Biochim Biophys Acta* **2009**; 1794(11):1549–1557. doi: 10.1016/j.bbapap.2009.06.023
 - Islam MM, Sonu VK, Gashnga PM, Moyon NS, Mitra S. Caffeine

- and sulfadiazine interact differently with human serum albumin: a combined fluorescence and molecular docking study. *Spectrochim Acta A Mol Biomol Spectrosc* **2016**;152: 23–33. doi: 10.1016/j.saa.2015.07.051
41. Cheng S, Song W, Yuan X, Xu Y. Gorge motions of acetylcholinesterase revealed by microsecond molecular dynamics simulations. *Sci Rep* **2017**; 7(1):3219. doi: 10.1038/s41598-017-03088-y
 42. Abraham MJ, Murtola T, Schulz R, Pall S, Smith JC, Hess B, et al. GROMACS: High performance molecular simulations through multi-level parallelism from laptops to supercomputers. *SoftwareX* **2015**;1(2):19–25. doi: 10.1016/j.softx.2015.06.001
 43. Bussi G, Donadio D, Parrinello M. Canonical sampling through velocity rescaling. *J Chem Phys* **2007**; 126(1):014101. doi: 10.1063/1.2408420
 44. Berendsen HJC, Postma JPM, van Gunsteren WF, DiNola A, Haak JR. Molecular dynamics with coupling to an external bath. *J Chem Phys* **1984**; 81(8):3684–3690. doi: 10.1063/1.448118
 45. Van der Spoel D, Lindahl E, Hess B, Groenhof G, Mark AE, Berendsen HJ. GROMACS: Fast, Flexible and Free. *J Comp Chem* **2005**;26:1701–1718. doi: 10.1002/jcc.20291
 46. Páll S, Hess B. A flexible algorithm for calculating pair interactions on SIMD architectures. *Comput Phys Commun* **2013**;184(12):2641–2650. doi: 10.1016/j.cpc.2013.06.003
 47. Yesylevskyy SO, Hushcha TO. Conformational relaxations of human serum albumin studied by molecular dynamics simulations with pressure jumps. *Biopolymers and Cell* **2012**; 28(6):486–492.
 48. Trott O, Olson AJ. AutoDock Vina: Improving the speed and accuracy of docking with a new scoring function, efficient optimization, and multithreading. *J Comp Chem* **2010**;31(2):455–461. doi: 10.1002/jcc.21334
 49. Pettersen EF, Goddard TD, Huang CC, Couch GS, Greenblatt DM, Meng EC, et al. UCSF Chimera—a visualization system for exploratory research and analysis. *J Comp Chem* **2015**; 25: 1605–1612. doi: 10.1002/jcc.20084
 50. Laskowski RA, Swindells MB. LigPlot+: multiple ligand–protein interaction diagrams for drug discovery. *J Chem Inf Model* **2011**; 51: 2778–2786. doi: 10.1021/ci200227u
 51. Yesylevskyy SO. Pteros: Fast and easy to use open-source C++ library for molecular analysis. *J Comp Chem* **2012**;33(19): 1632–1636. doi: 10.1002/jcc.22989
 52. Yesylevskyy SO. Pteros 2.0: Evolution of the fast parallel molecular analysis library for C++ and python. *J Comp Chem* **2015**;36(19):1480–1488. doi: 10.1002/jcc.23943
 53. Taverna M, Marie AL, Mira JP, Guidet B. Specific antioxidant properties of human serum albumin. *Ann Intensive Care* **2013**;3(1); 4. doi: 10.1186/2110-5820-3-4
 54. Sobhani R, Pal AK, Bhattacharjee A, Mitra S, Aguan K. Screening Indigenous Medicinal Plants of Northeast India for Their Anti-Alzheimers Properties. *Pharmacogn J* **2017**;9 (1): 46–54. doi: 10.5530/pj.2017.1.9
 55. Sánchez-Linares I, Pérez-Sánchez H, Cecilia JM, García JM. High-throughput parallel blind virtual screening using BINDSURE. *BMC Bioinformatics* **2012**;13 Suppl 14:S13. doi: 10.1186/1471-2105-13-S14-S13.
 56. Pajouhesh H, Lenz GR. Medicinal chemical properties of successful central nervous system drugs. *Neurotherapeutics* **2005**;2: 541–553. doi: 10.1602/neurorx.2.4.541
 57. Cornish-Bowden A. *Inhibitors and Activators of Enzyme Kinetics*. Butterworth-Heinemann; **1979**. p. 73–98.
 58. Dvir H, Silman I, Harel M, Rosenberry TL, Sussman JL. Acetylcholinesterase: From 3D Structure to Function. *Chem Biol Interact* **2010**;187 (1–3): 10–22. doi: 10.1016/j.cbi.2010.01.042
 59. Baruah P, Basumatary G, Yesylevskyy SO, Aguan K, Bez G, Mitra S. Novel coumarin derivatives as potent acetylcholinesterase inhibitors: insight into efficacy, mode and site of inhibition. *J Biomol Struct Dyn* **2018**, doi: 10.1080/07391102.2018.1465853.
 60. de Souza LG, Rennä MN, Figueroa-Villar JD. Coumarins as cholinesterase inhibitors: a review. *Chem Biol Interact* **2016**;254: 11–23. doi: 10.1016/j.cbi.2016.05.001
 61. De Ferrari GV, Mallender WD, Inestrosa NC, Rosenberry TL. Thioflavin T. Is a fluorescent probe of the acetylcholinesterase peripheral site that reveals conformational interactions between the peripheral and acylation sites. *J Biol Chem* **2001**;276 (26): 23282–23287. doi: 10.1074/jbc.M009596200
 62. Islam MM, Mitra S. Cholinergic Inhibitors Replace Thioflavin-T from Acetylcholinesterase Binding Pocket: A Potential Fluorescence Based Molecular Switch. *Chem Phys Lett* **2016**;664: 63–69. doi: 10.1016/j.cplett.2016.09.079
 63. Islam MM, Rohman MA, Gurung AB, Bhattacharjee A, Aguan K, Mitra S. Correlation of cholinergic drug induced quenching of acetylcholinesterase bound thioflavin-T fluorescence with their inhibition activity. *Spectrochim Acta A Mol Biomol Spectrosc* **2018**;189:250–257. doi: 10.1016/j.saa.2017.08.009
 64. Bajda M, Więckowska A, Hebda M, Guziar N, Sotriffer CA, Malawska B. Structure-Based Search for New Inhibitors of Cholinesterases. *Int J Mol Sci* **2013**;14 (3): 5608–5632. doi: 10.3390/ijms14035608
 65. Imramovsky A, Stepankova S, Vanco J, Pauk K, Monreal-Ferriz J, VinSova J, et al. Acetylcholinesterase-Inhibiting Activity of Salicylanilide N-Alkylcarbamates and Their Molecular Docking. *Molecules* **2012**; 17: 10142–10158. doi: 10.3390/molecules170910142
 66. Colletier JP, Fournier D, Greenblatt HM, Stojan J, Sussman JL, Zaccai G, et al. Structural Insights into Substrate Traffic and Inhibition in Acetylcholinesterase. *EMBO J* **2006**;25(12): 2746–2756. doi: 10.1038/sj.emboj.7601175
 67. Nawaz SA, Ayaz M, Brandt W, Wessjohann LA, Westermann B. Cation- π and π - π Stacking Interactions Allow Selective Inhibition of Butyrylcholinesterase by Modified Quinine and Cinchonidine Alkaloids. *Biochem. Biophys Res Commun* **2011**;404(4): 935–940. doi: 10.1016/j.bbrc.2010.12.084
 68. Deb PK, Sharma A, Piplani P, Akkinepally RR. Molecular Docking and receptor-specific 3D-QSAR studies of acetylcholinesterase inhibitors. *Mol Divers* **2012**;16(4): 803–823. doi: 10.1007/s11030-012-9394-x